VLBA Imaging of the Blazar, J08053+6144

Daniel Zirzow* Jeffrey Karle † Joe Craig ‡

May 11, 2009

Contents

*University of New Mexico, 1009 Bradbury, Albuquerque, NM 87131 USA. E-mail: dzirzow@unm.edu

†E-mail: jeffrey.karle@gmail.com

‡E-mail: joecraig@unm.edu

Abstract

We present observations of the high redshift ($z = 3.03$) blazar J08053+6144 at both 5 GHz and 15 GHz using the VLBA. We obtained high dynamic range Stokes I maps of J08053+6144 at 5 and 15 GHz. Polarization maps plotting source intensity (Stokes I) and polarization angle are included with a rotation measure map. Using data obtained from our VLBA observations we provide calculations for the spectral index α that characterizes the source emission ($\epsilon_\nu \propto \nu^\alpha$). We also calculate the brightness temperature of the source at 5 and 15 GHz. The magnetic field strength is also calculated using a method mentioned by Miley (1980) [1] under the conditions that we are solving for a minimum energy condition $u_{me} = (\frac{7}{3})(\frac{{B_{me}}^2}{8\pi})$. We also compare our observations with observations of this source at 5 GHz in 1998 (Taylor, *et al*) [2] in order to look for bulk motion within the visible jet component of the source.

1 Introduction

Blazars are among the most energetic sources in the observable Universe. Blazars emit radiation throughout the entire electromagnetic spectrum from Gamma Rays to Radio. Blazars are a type of radio-loud Active Galactic Nuclei (AGN) in which the relativistic jet that is responsible for the vast majority of non-thermal emission is oriented at a very small angle with respect to our line of sight. Though a wide variety of blazar properties can be explained by the existence of relativistic jets, understanding how jets form is still an unsolved problem in astrophysics. Relatively recent magnetohydrodynamic (MHD) numerical simulations lend support to the theory that relativistic jets form in environments containing magnetized gas flowing around a supermassive black hole that lies at the center of AGNs. It is believed that the difference between radio-loud and radio-quiet AGN can be attributed to differences in spin of the supermassive black hole. Radio-loud sources seem to be associated with Kerr holes and radio-quiet sources with Schwarzschild holes that are of order 2-4 times weaker than their radio-loud counterparts [3]. Recent data also supports the shock in jet model in which primary emission is from shock waves that move through the jet, rather than the jet being comprised of a homogenous plasma [4].

Blazar emission typically exhibits two generally broad components, one that peaks somewhere from the infrared to X-rays and the other that peaks in the MeV to TeV energy range [5]. Blazars commonly exhibit variability at all wavelengths at which they radiate, though these variations take place on different timescales ranging from years to less than a day [6]. The most extreme variability takes places in the γ-rays with very short periods of variation. The most luminous sources have γ-ray luminosities as high as 1049 ergs $\cdot$ s^{-1} [7]. It is believed that the γ-ray emission emanates from the jet and not the core. There are two classes of models that attempt to explain the nature of the γ-ray emission, namely hadronic and leptonic, depending on whether protons or electrons are primarily responsible for the γ-ray emission. It is currently believed that the primary source of γ-ray emission is due to inverse Compton scattering involving leptonic processes [4]. By the process of inverse Compton scattering a photon with frequency ν_0 will scatter off an electron with a Lorentz factor $\gamma = m_e c^2/E$ with a final frequency $\nu_f = (4/3)\gamma^2\nu_0$ [8]. Because blazars emit extremely large quantities of γ-rays they dominate the sky at high energies. A vast majority of the high energy sources detected by EGRET (The Energetic Gamma Ray Experiment Telescope) are blazars.

2 Calibration of VLBA Data

Calibration and imaging of our VLBA data for J08053+6144 was done in both AIPS and difmap. Upon receiving our data initial calibration in AIPS was performed. Using the two multi source data files at 5 and 15 GHz, we ran the tasks SPLIT and FITTP to create single source data files in Stokes RR for both the target source and our calibrators. Our calibration sources included 3C84, 3C279, J1310+3220, and J0854+2006. Once we had single source data sets in RR we performed imaging and self calibration in difmap. Once we had achieved acceptable images of theses sources we saved the images and models and read them back into AIPS individually using the task IMLOD. We then used our images of all 5 sources to perform calibration at both 5 and 15 GHz using our models from difmap instead of a simple point source model. A point source model would not suffice as all of the sources were at least partially resolved. Once we had a better calibration of the data at both frequencies we wrote out Stokes I files for our target source J08053+6144 to image in difmap.

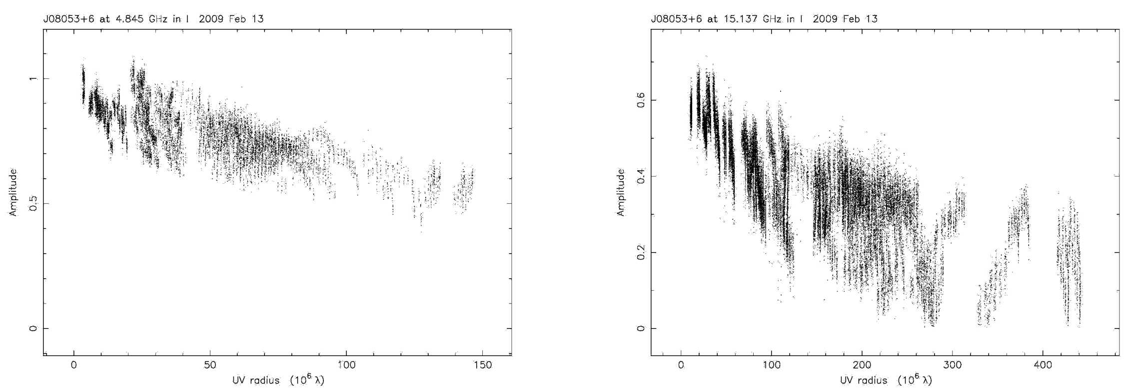

(a) 5 GHz

(b) 15 GHz

Figure 1: Rad plots

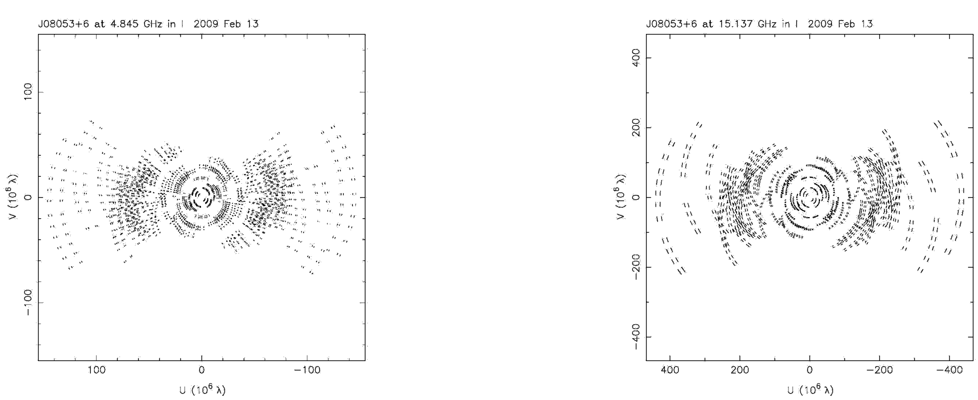

(a) 5 GHz

(b) 15 GHz

Figure 2: UV plots

3 Imaging J08053+6144 at 5 GHz & 15 GHz

We made Stokes I maps of J08053+6144 at both 5 and 15 GHz. Imaging was performed in difmap. Using the EVN Calculator for the VLBA we calculated theoretical noise at 5 GHz with 228 minute total scan duration is 0.071 mJy/Beam, and 0.123 mJy/Beam at 15GHz with 236 minute scan duration. At 5 GHz our Stokes I map has an off source noise level of 0.12 mJy/Beam and a peak value of 789.89 mJy/Beam. At 15 GHz the Stokes I map achieved an off source noise level of 0.15 mJy/Beam and a peak value of 356.38 mJy/Beam with a 236 minute total scan duration.

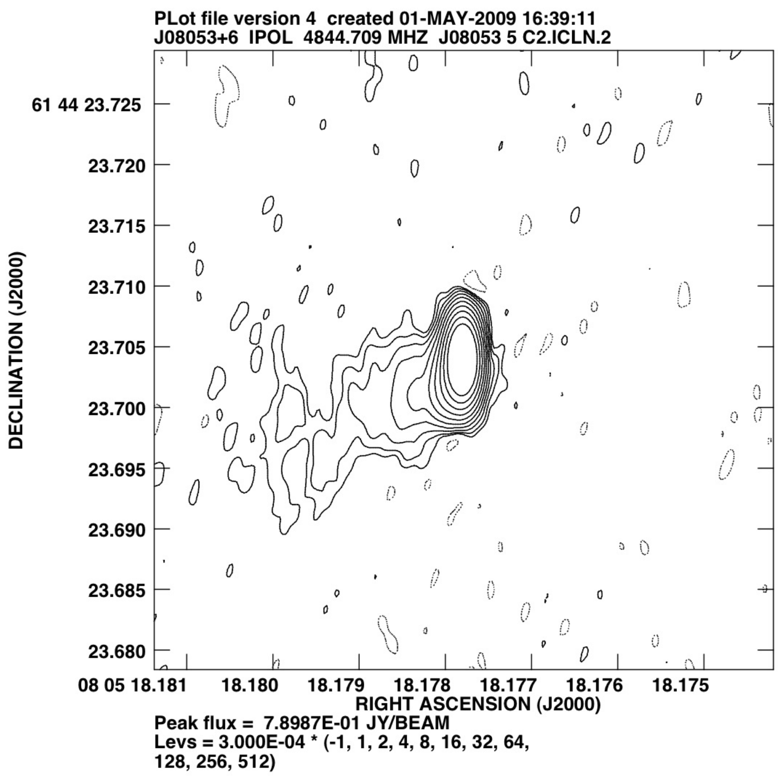

Figure 3: Contour Image, 5 GHz

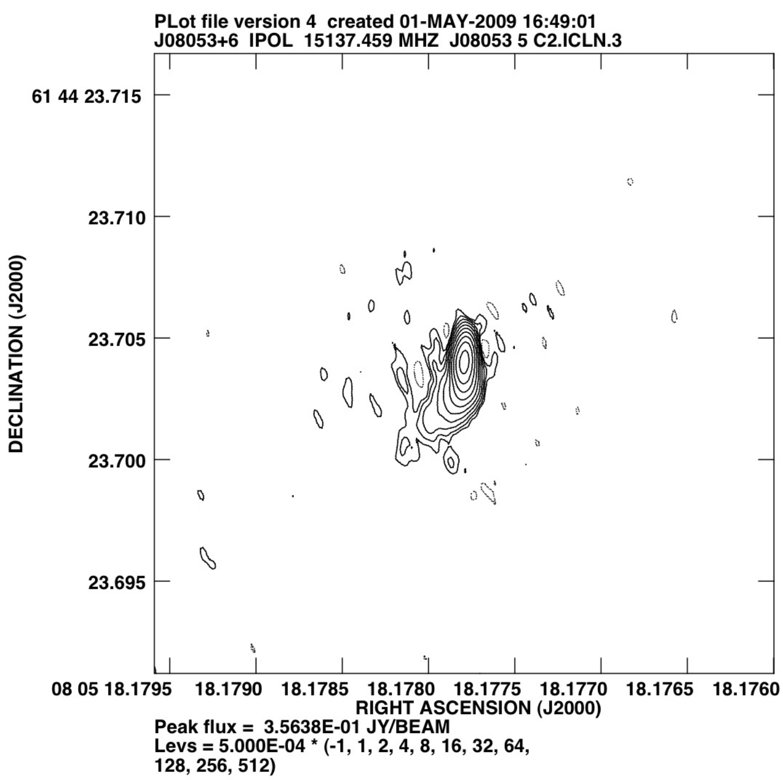

Figure 4: Contour Image, 15 GHz

4 Model Fitting

From model fitting in difmap with a model consisting of three two-dimensional Gaussian components, we obtained total flux values of 0.774 Jy, 0.1250 Jy, and 0.0310 Jy, each with respective sizes of 0.416 milliarcsec x 0.416 milliarcsec, 0.00 milliarcsec x 1.572 milliarcsec, and 3.24 milliarcsec x 6.951 milliarcsec. Our model was a fairly reasonable fit to the observed source structure. During the model fitting process in difmap we reached a Chi-squared value of ≈ 1. The core of J08053+6144 was modeled as a very compact, near circular component while the jet was best modeled with a much larger Gaussian component. Model fitting at 15 GHz was also done, but 4 Gaussian components were needed and the best fit yielded a Chi-squared value of ≈ 1.95. The central component of the model that simulated the core was forced to remain circular. The size of the core model component at 15 GHz had an angular size of 0.16 milliarcsec. Some model fitting was conducted using the available calibrated data of J08053+6144 from the 1998 observation in order to see if there was any bulk motion within the jet component of the emission. With the observed data we see very negligible motions of the jet under the current model.

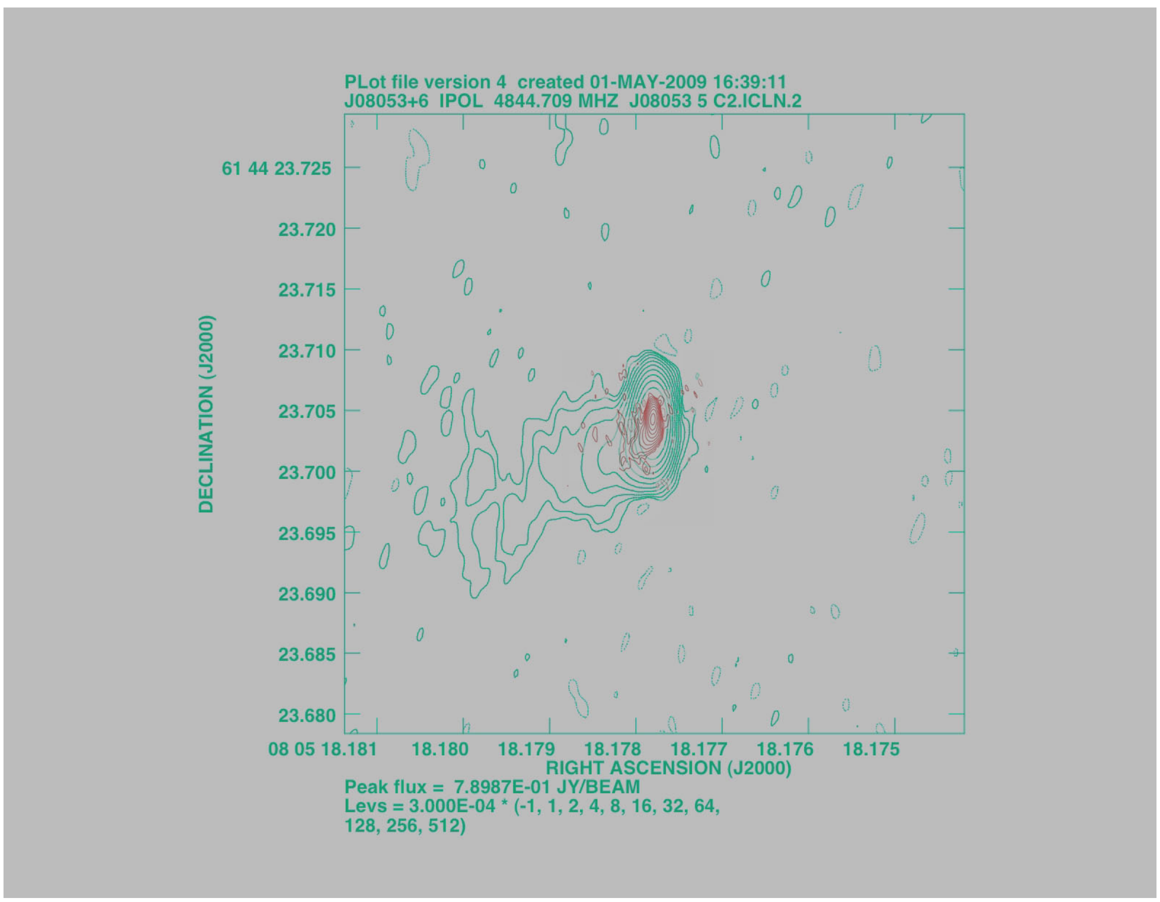

Figure 5: Combined 5 GHz (blue) and 15 GHz (red) contour maps.

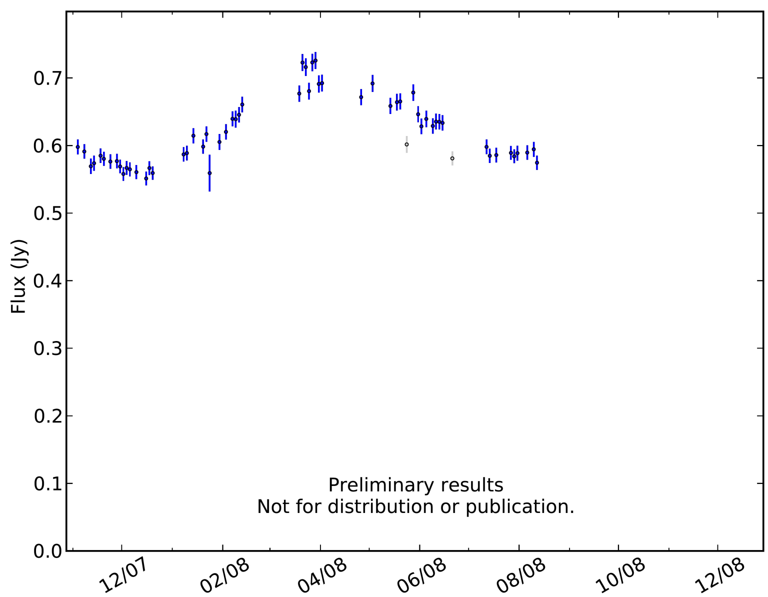

Figure 6: Variation in the flux of J08053+6144 over time.

5 Polarization

Polarization describes the orientation of the oscillations inherent in electric and magnetic fields, and is a fundamental property of sources of synchrotron radiation. Conventionally, polarization is labeled by specifying the direction of the electric field, which may be oriented in a single direction indicating linear polarization, or it may rotate as it propagates, exhibiting elliptical polarization. There exists an orthogonal state to each polarization, and incoherent light may contain many polarization states. To describe polarized light, the Stokes Parameters are identified using the perpendicular components of the electric field normal to the propagation direction,

$$E_x = e_{x(t)} \times cos(\omega t + \delta_x) \tag{1}$$

$$E_y = e_{y(t)} \times cos(\omega t + \delta_y) \tag{2}$$

With these, the common parameters are,

$$I = |e_x^2(t)| + |e_y^2(t)| \tag{3}$$

$$Q = |e_x^2(t)| - |e_y^2(t)| \tag{4}$$

$$U = 2|e_x(t)e_y(t)cos(\delta_x - \delta_y)| \tag{5}$$

$$V = 2|e_x(t)e_y(t)sin(\delta_x - \delta_y)| \tag{6}$$

For telescopes such as the VLA, circular polarized feeds are used, and the Stokes parameters can be described by,

$$\begin{gathered} \mathrm{I} = \mathrm{RR} + \mathrm{LL} \\ \mathrm{Q} = \mathrm{RL} + \mathrm{LR} \\ \mathrm{U} = i(\mathrm{LR} - \mathrm{RL}) \\ \mathrm{V} = \mathrm{LL} - \mathrm{RR} \end{gathered}$$

From these parameters, the polarization angle and intensity can be determined from,

$$\phi = 0.5\, atan(U/Q) \tag{7}$$

$$p = \sqrt{Q^2 + U^2} \tag{8}$$

	VLBA IF 1, 2					VLBA IF 3, 4					VLA			Dif 1,2	Dif 3,4
Source	I	Q	U	p	ϕ	I	Q	U	p	ϕ	I	p	ϕ		
J1310	920	-6.4	0.76	6.5	87°	912	-0.27	-1.2	1.23	-51°	1000	17	23°	-64°	74°
3C279	9300	134	24	136	5°	9300	82.3	-9.5	82.8	-3.29°	10200	150	116°	-69°	119°
J0854	1500	-4.2	2.78	5	73.2°	1500	-0.61	0.39	0.72	73.7°	1690	56.7	-78°	-151.7°	-151.7°

Table 1: Polarization Calibrator Comparison

Corruption of the polarization signal can be due to the atmosphere, instrumental gain variations, and instrumental imperfections. To correct for this, astronomical calibration sources are chosen that generally exhibit synchrotron emission with significant linear polarization and weak circular polarization. Calibration for the polarization was performed using difmap to create two Stokes I maps each for the target source and three calibrator sources, J0854, 3C279, and J1310. For each source, a map was created for IF 1 and 2, and also for IF 3 and 4. Following this, a similar procedure of 'clean' and 'keep' iterations for each source produced clean maps in Q and U for each IF pair. These Q and U maps were then read back into AIPS with IMLOD, and the IMEAN task derived the total flux in I, Q, and U for each IF pair. Utilizing the above equations for the calibrators' polarization intensity and polarization angle, our results were compared with previous VLA observations to determine the difference in polarization angle and select which calibrators would be most useful for applying to our target source.

For IF 1 and 2, only the calibrator sources J1310 and 3C279 showed enough similarity in polarization angle difference to apply to our target source. Using CLCOR, we applied the calibration data to our target source, and imaged the polarization intensity and angle with PCNTR for each IF pair. The polarization maps indicate a relatively constant polarization angle throughout the central component of the source, with only minor polarized features in the observed jet appearing in the IF 3 and 4 map. The degree of polarization is determined by the ratio of the total flux intensity and the polarization intensity. For the target source, IMEAN obtained IF 1 and 2 values of 8.3 mJy and 41 mJy for Q and U, respectively, which yield a polarization intensity of 41.8 mJy. In IF 3 and 4, Q and U values were 2.3 mJy and 34 mJy, yielding an intensity of 34.1 mJy. Summing the model component flux density values achieved a total flux of 929.97 mJy, which allows the determination of the amount of polarization in each IF pair to be 22.25% for IF 1 and 2, and 27.27% in IF 3 and 4.

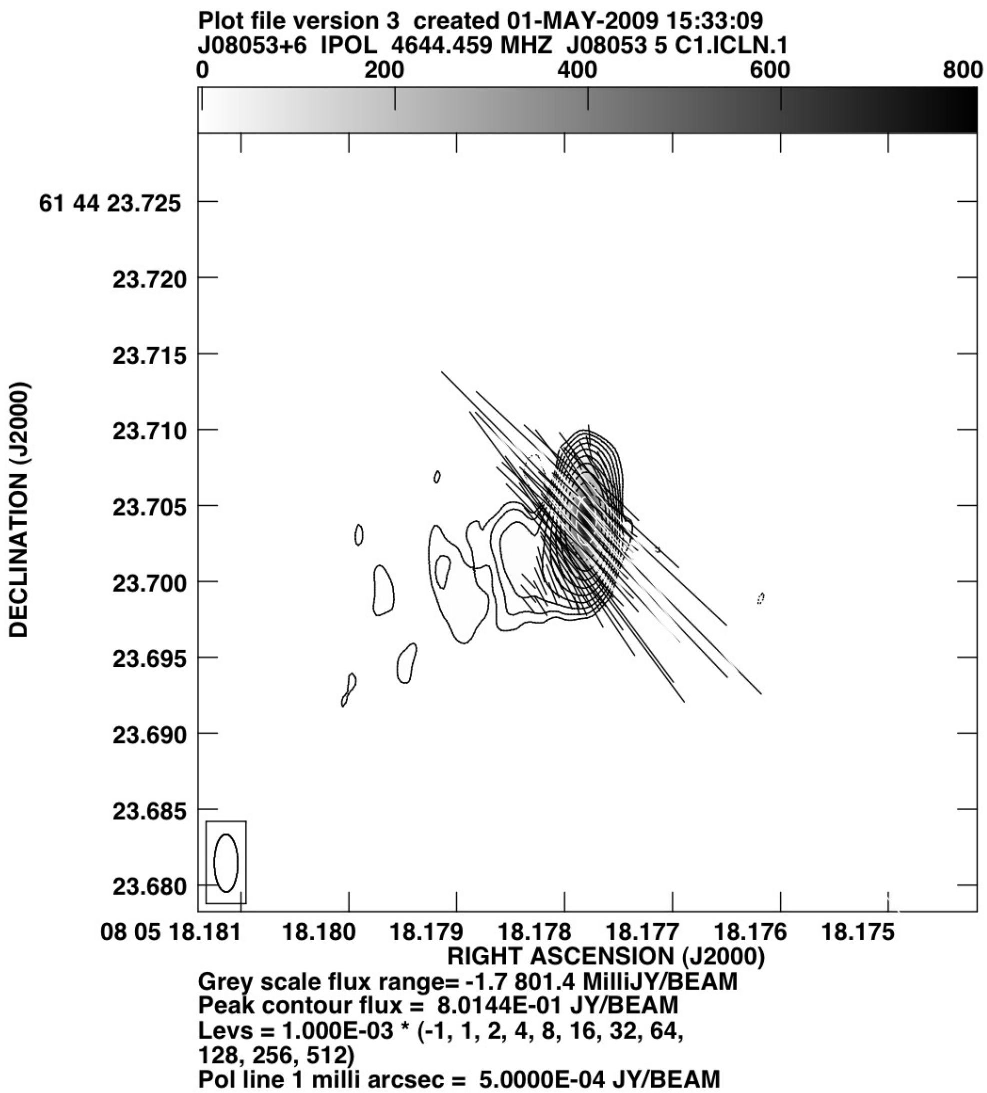

Figure 7: Polarization Contour Image 1, 5 GHz

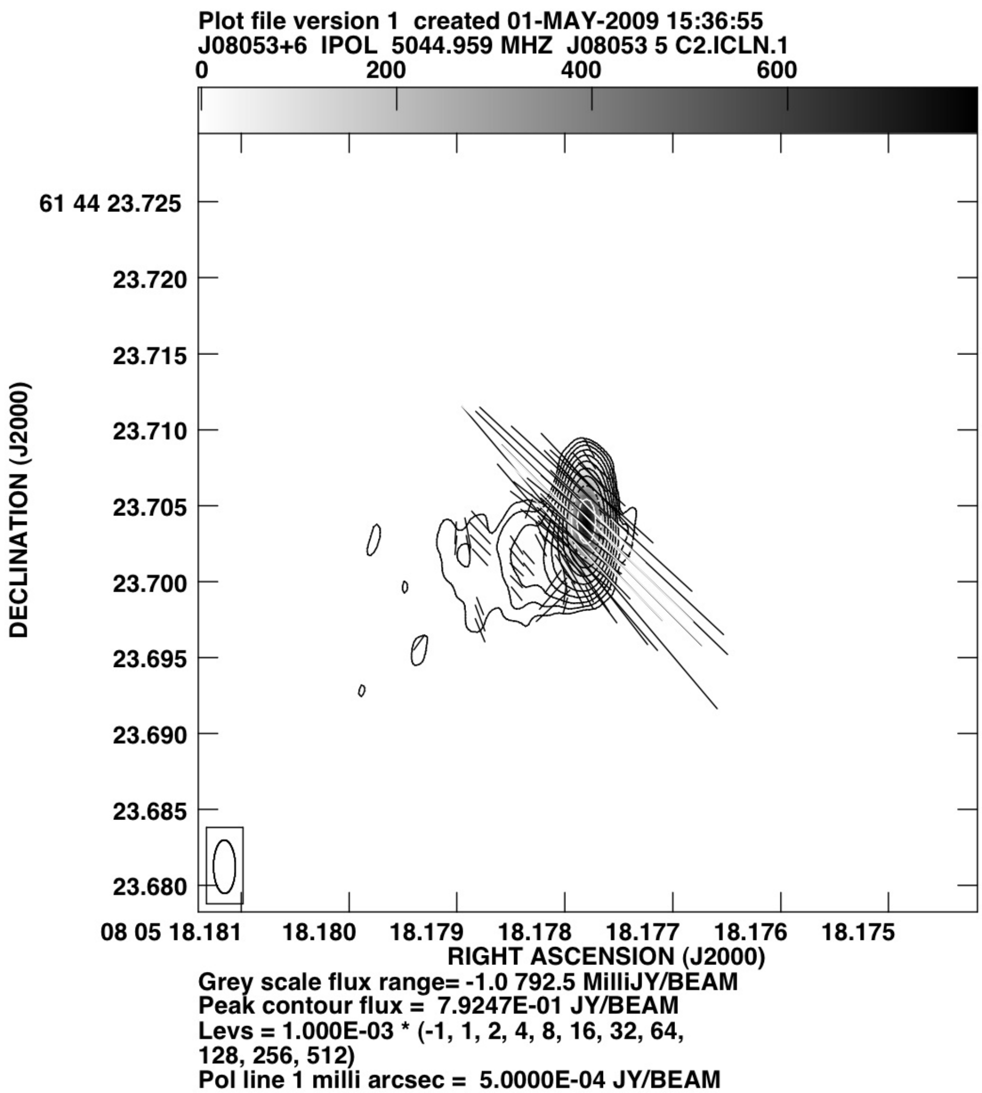

Figure 8: Polarization Contour Image 2, 5 GHz

6 Results and Analysis

Based our VLBA observations and the Stokes I maps that we generated, we were able to calculate some general source parameters. Using our model fit for the core component of J08053+6144 for the angular size of the source in arc seconds the brightness temperature, T_b, can be calculated for the core of the blazar.

$$T_b = \frac{S_\nu c^2}{2k\nu^2\theta^2} \tag{9}$$

where, S_ν is the frequency dependent flux density, θ is the angular resolution, k is Boltzmann's constant, and c is the speed of light.

Using the peak value of the Stokes I maps at 5 GHz and 15 GHz, using $\theta = 0.000416$" for the 5 GHz, and $\theta = 0.00016$" for the 15 GHz model we obtain:

$$T_{b,5GHz} = 2.516 \times 10^{11} \text{ K}$$

$$T_{b,15GHz} = 8.57 \times 10^{10} \text{ K}$$

Thus, it is apparent that the nature of the emission is non-thermal. If a power law spectrum is assumed ($\epsilon_\upsilon \propto \upsilon^\alpha$), the spectral index of the emission can be calculated using two known source flux densities at two different observational frequencies. Thus, α can be calculated using the very simple formula,

$$\alpha = \frac{log(S_{5\,GHz}/S_{15\,GHz})}{log(5\,GHz/15\,GHz)} \tag{10}$$

Using our peak Stokes I intensities at 5 and 15 GHz,

$$\alpha = \text{-0.724}$$

Another useful parameter to calculate if the minimum magnetic field strength that will give rise to the synchrotron radiation. Using the following equation for the minimum strength magnetic field [1] and using, $k = \eta = 1$, $z = 3.03$, $\alpha = -0.724$, $sin^{3/2}(\phi) = 1$, $\theta_x = \theta_y = 0.000416$", $F_0 = 0.78989$ Jy, $\nu_0 = 5$ GHz, $\nu_1 = 0.1$ GHz, $\nu_2 = 100$ GHz, and $s = 0.008$ kpc.

$$\upsilon_{me} = (7/3)(B_{me}^2/8\pi) = 0.0928\, B_{me}^2\, erg\, cm^{-3} \tag{11}$$

where the corresponding magnetic field is

$$B_{me} = 5.69 \times 10^{-5} \left[\frac{(1+k)}{\eta}(1+z)^{3-\alpha} \frac{1}{\theta_x\theta_y\, s\, sin^{3/2}(\phi)} \times \frac{F_0}{\nu_0^\alpha} \frac{\nu_2^{\alpha+1/2} - \nu_1^{\alpha+1/2}}{\alpha + \frac{1}{2}} \right]^{2/7} gauss \tag{12}$$

Here k is the ratio of energy in the heavy particles to that in the electrons, η is the filling factor of the emitting regions, z is the redshift, θ_x and θ_y (arcsec) correspond either to the source/component sizes or to the equivalent beam widths, s (kiloparsec) is the path length through the source in the line of sight, ϕ is the angle between the uniform magnetic field and the line of sight, F_0 (Jy or Jy per beam) is the flux density or brightness of the region at frequency ν_0 (GHz), ν_1 and ν_2 (GHz) are the upper and lower cut off frequencies presumed for the radio spectrum, and α is the spectral index [$F(\nu) \propto \nu^\alpha$, $\nu_1 < \nu < \nu_2$].

We obtain a minimum magnetic field strength of $\approx$ 224.6 mGauss.

7 Relativisitic Beaming

Relativistic beaming is the process by which the relativistic effect modifies the apparent luminosity of a relativistic jet. Beaming occurs in AGN where a central supermassive black hole is the source of energy for the jets of intensely energetic plasma. Electrons inside the jet travel at speeds just a tiny fraction below the speed of light and are whipped around by the magnetic field. Each change in direction by an electron is accompanied by the release of energy in the form of a photon (resulting in synchrotron emission). In the rest frame of the Earth, the radiation is approaching at speeds which can be in the range of 95% to 98% of the speed of light, and because of Special Relativity, the luminosity observed on Earth will be higher than the intrinsic luminosity measured in the rest frame of the jet. This is especially true for Blazars, in which the jets are directed towards Earth.

In the simple jet model of a single homogeneous sphere the observed luminosity is related to the intrinsic luminosity by:

$$S_0 = S_e D^{3-\alpha} \tag{13}$$

where, S_0 is the observed luminosity; S_e is the intrinsic luminosity (aka emitted luminosity); α is the spectral index; and D is the Doppler factor, which depends on the speed of the jet and the angle to the line of sight.

The beaming equation can be broken down into a series of three effects:

- Relativistic Abberation, which accounts for a change in luminosity of D^2.
- Time Dilation, which accounts for a change in luminosity of D.
- Blue/Red Shifting, which changes the observed luminosity at a particular frequency and accounts for a change in luminosity of $1/D^{\alpha}$.

The Doppler factor is dependent on the Lorentz factor, γ, the relativistic beta, $\beta = v_j/c$ (where v_j is the speed of the jet, and θ (the jet's angle to the observed line of sight on Earth) by:

$$D = \frac{1}{\gamma(1 - \beta cos\theta)} \tag{14}$$

Since θ is relatively difficult to determine, we have plotted the Doppler factor for a range of angles (figure 9), assuming $\gamma = 5$ (98% speed of light).

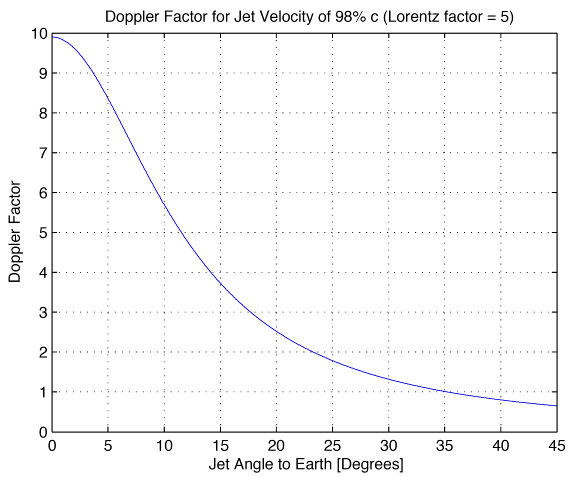

(a) Doppler factor as a function of jet angle

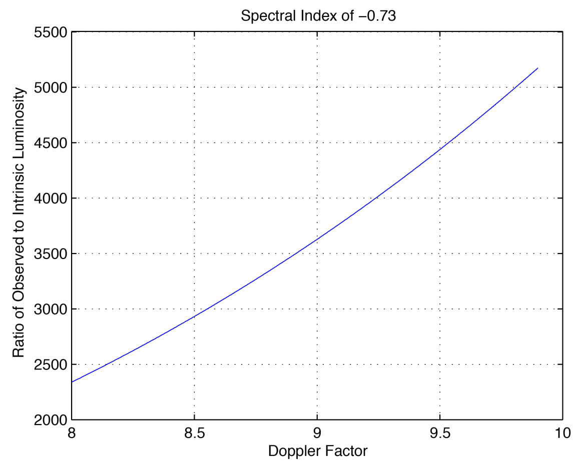

(b) Ratio of observed to intrinsic luminosity for a range of Doppler factors

Figure 9: Relativistic beaming effects for J08053+6144

Assuming the blazar J08053+6144 has a θ between $0°$ and $5°$, figure 9 (b) shows an increase in observed to intrinsic luminosity of between 2000 and 5000 times. These results are interesting because we get a huge amplification of the intrinsic luminosity from relativistic beaming for AGN which have their jets directed towards Earth. If the same source, J08053+6144, were actually not a Blazar and had jets at a $45°$ angle to Earth, the VLBA would not be sensitive enough to observe the emission.

To get the intrinsic luminosity of the jet, we use the measured flux, and our distance from the source. If we assume the source is a sphere[1], luminosity is related to flux by:

$$Flux = \frac{Luminosity}{4\pi d^2} \tag{15}$$

where d is the distance from the source to the observer (for J08053+6144, $z = 3.033$, $d = 4.24$ Gpc).

Using $Flux = 0.774\ Jy = 0.774 \cdot 10^{-23} erg \cdot sec^{-1} \cdot cm^{-2}$, we obtain an observed luminosity of $1.75 \cdot 10^{-3} erg \cdot sec^{-1}$. Using the results from relativistic beaming above, we can say the intrinsic luminosity of the source is roughly $5 \cdot 10^{-7} \cdot erg \cdot sec^{-1}$.

[1]The blazar jet is certainly not a sphere, but for the simple purpose of illustrating the calculation for luminosity, we assume a spherical cow, or cat; whichever is prefered.

8 Faraday Rotation

Faraday rotation is a phenomenon by which the polarization angle of light rotates in the presence of a magnetic field that has some component oriented parallel to the propagation direction of the light. This effect was first discovered by Michael Faraday in 1845, and was essentially the first experimental evidence that light and electromagnetism are in fact related.

In astrophysics, Faraday rotation is induced by free electrons in the interstellar medium lying between the Earth and any source we wish to observe. In such an environment, Faraday rotation is dependent on only three parameters; the wavelength of the light, the electron density, and the component of the magnetic field that is oriented parallel to the propagation direction of the light.

We have the following relationship between the polarization angles:

$$\Psi = \Psi_0 + RM\,\lambda^2 \tag{16}$$

where Ψ_0 is the initial polarization angle and Ψ is the angle after rotation.

The Rotation Measure RM can be expressed in CGS units as:

$$RM = \frac{e^3 \int_0^s \eta_e B\,ds}{2\pi m^2 c^4} \tag{17}$$

We produced a Faraday rotation Measure map using the polarization angle maps for IF 1,2 and IF 3,4. Using the task COMB in AIPS we created a basic rotation measure map of the source. In this map one can see that there is a non-zero rotation of the polarization angle. Also observed is a small gradient in the rotation measure across the source.

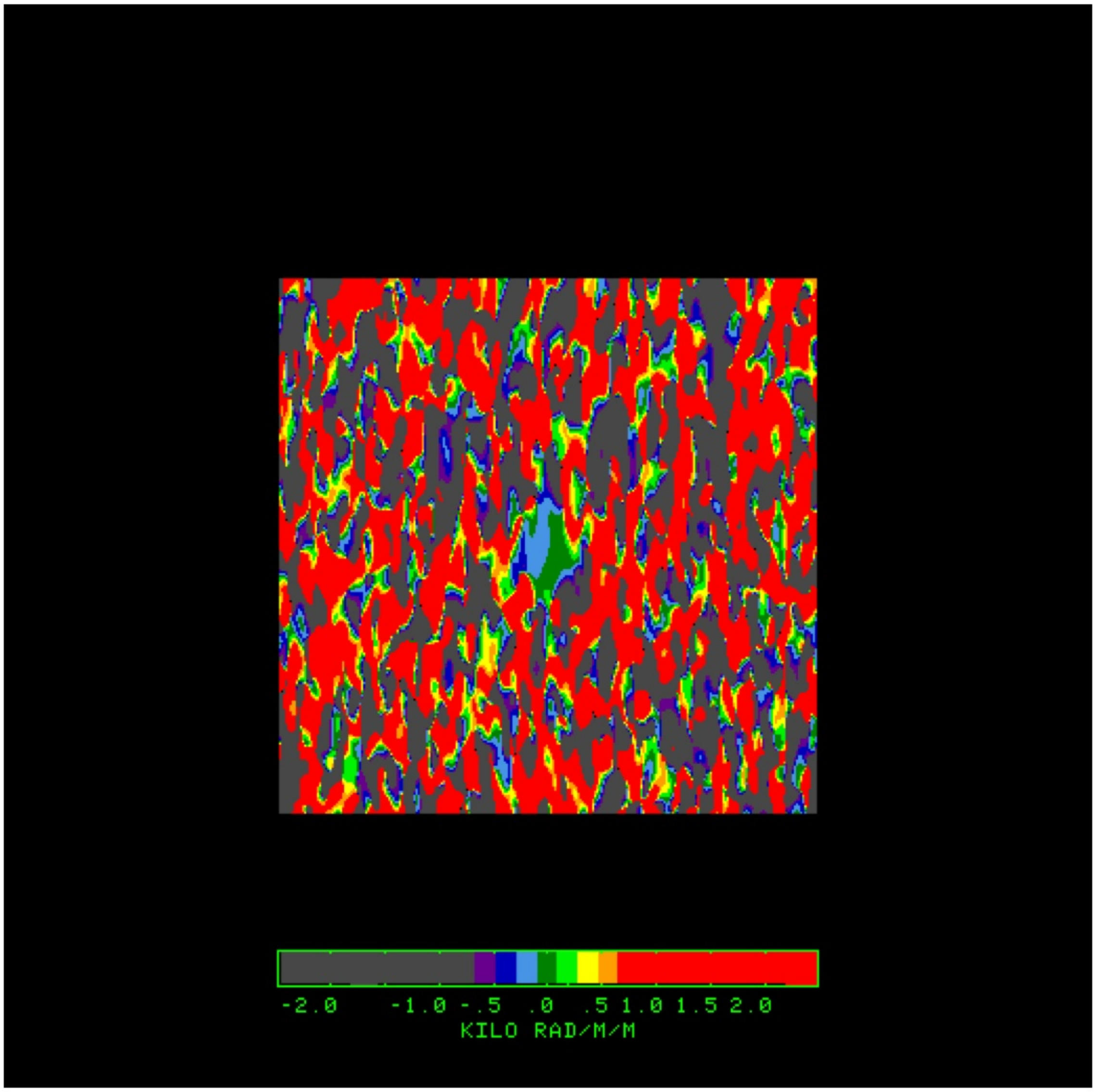

Figure 10: Rotation Measure Map, 5 GHz

9 Conclusion

The blazar J08053+6144 was imaged with VLBA at 5 GHz and 15 GHz. Calculations for flux density, brightness temperature, and polarization have been provided. Since blazars are highly variable radio sources, it might be of interest to observe this source over time to get a better understanding of the variations in the jet's luminosity. Some futher analysis of polarization might also yield interesting results.

References

[1] Miley, G., The Structure of Extended Extragalactic Radio Sources, Ann. Rev. Astron. Astrophys. 1980, 182-183.

[2] Taylor, G. B. et al. VIPS Observation of J08053+6144, 1998, http://www.phys.unm.edu/ gb-taylor/VIPS/vipsdat/J08053+6144.shtml.

[3] Meier, D. L., Simulations of Relativistic Jet Formation in Radio Sources, ASP, 2001.

[4] Mastichiadis, A. et al., Models of Variability in Blazar Jets, ASA, 2002.

[5] Sikora, M. et al., Blazars, American Institute of Physics, 2001.

[6] Böttcher, M., Modeling the Emission Processes in Blazars, Astrophysics and Space Science, 2006.

[7] Ghisellini, G. et al., The Blazar Sequence: A New Perspective, RAS, 2008.

[8] Daly, R. A., Inverse Compton Scattering and the Alignments Observed In High Redshift Radio Galaxies, APJ, 1992.